

Article

Fano Resonance Enhanced Nonreciprocal Absorption and Scattering of Light

Ben Hopkins ^{1,*}, Andrey E. Miroschnichenko ¹, Alexander N. Poddubny ^{2,3} and Yuri S. Kivshar ^{1,3}

¹ Nonlinear Physics Centre, Australian National University, Canberra ACT 2601, Australia; E-Mails: andrey.miroschnichenko@anu.edu.au (A.E.M.); ysk@internode.on.net (Y.S.K.)

² Ioffe Physical-Technical Institute of the Russian Academy of Sciences, St. Petersburg 194021, Russia; E-Mail: poddubny@coherent.ioffe.ru

³ ITMO University, St. Petersburg 197101, Russia

* Author to whom correspondence should be addressed; E-Mail: ben.hopkins@anu.edu.au.

Received: 17 May 2015 / Accepted: 18 June 2015 / Published: 22 June 2015

Abstract: We reveal that asymmetric plasmonic nanostructures can exhibit significantly different absorption and scattering properties for light that propagates in opposite directions, despite the conservation of total extinction. We analytically demonstrate that this is a consequence of nonorthogonality of eigenmodes of the system. This results in the necessity for modal interference with potential enhancement via Fano resonances. Based on our theory, we propose a stacked nanocross design whose optical response exhibits an abrupt change between absorption and scattering cross-sections for plane waves propagating in opposite directions. This work thereby proposes the use of Fano resonances to employ nanostructures for measuring and distinguishing optical signals coming from opposite directions.

Keywords: fano resonance; plasmonics; stereometamaterials; nanophotonics; reciprocity

1. Introduction

Reciprocity is one of the key concepts in optics because it is related to the equal transmission of oppositely-propagating plane waves through any structure or medium; a manifestation of the total optical loss being conserved [1–4]. Indeed, to induce a difference in transmission from oppositely-propagating

light requires optical elements that are driven by magnetic fields or materials to break the conditions of reciprocity [5–8]. Such nonreciprocal optical behavior is widely utilized in optical communications devices, and particularly optical isolators and circulators. There has subsequently been significant interest in miniaturizing these devices for incorporation into nanophotonic chips and the broader realization of integrated optics systems. However, there remain limitations on the minimum propagation length or interaction time that is needed to produce sufficient reciprocity breaking. Promising avenues exist to utilize gyromagnetic response [9] or engineered nonlinearity [10] to inherently break reciprocity, but here we instead present a way to produce nonreciprocal optical behavior in a linear system without breaking reciprocity. We begin by acknowledging that nanoantennas and metasurfaces, in general, have *two* separate loss channels: the radiative loss (scattering cross-section) and the dissipative material loss (absorption cross-section), both of which can be associated with distinct and measurable quantities. In particular, we show that the reciprocity constraint is not directly applicable to these *independent* loss channels. Indeed, this freedom has recently been demonstrated to allow circular dichroism in the absorption of planar structures [11] (arXiv). Here, we extend this approach to investigate nonreciprocal absorption and scattering cross-sections of three-dimensional nanostructures and stereometamaterials. First, we show that existence of nonorthogonal eigenmodes, in general, results in resonant interference phenomena associated with the Fano resonances. We then demonstrate that this nonorthogonality permits the absorption and scattering cross-section of an optical device to distinguish between opposite propagation directions, such as depicted in Figure 1.

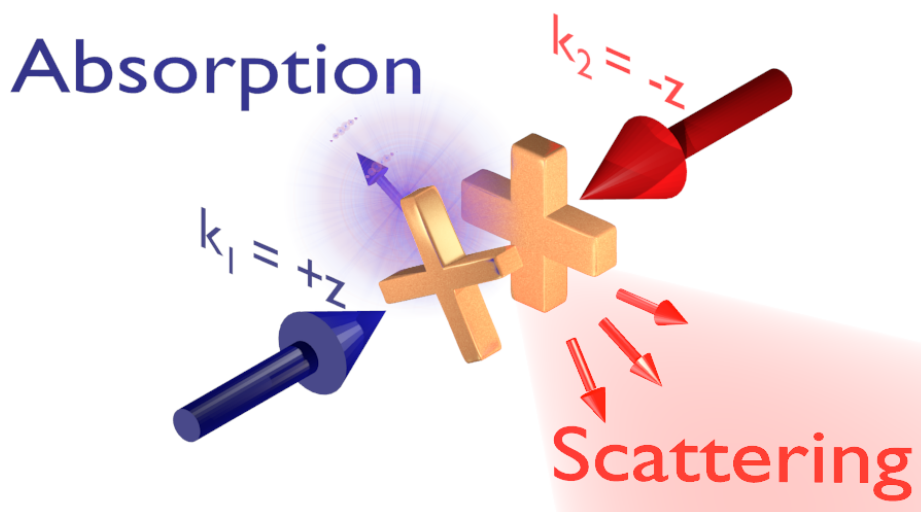


Figure 1. A schematic representation of different optical loss channels: radiative (scattering) and dissipative (absorption). A planewave propagating in one direction will be channeled into far field scattering, while (simultaneously) an identical plane wave propagating in the opposite direction will be channeled into material absorption.

It suggests that absorption and scattering provide us with the independent measurements on oppositely-propagating signals in the vicinity of a Fano resonance. We further show that such a nonreciprocal optical device can be designed in a way to have optical response being independent of polarization. This behavior demonstrates that direction-isolating measurements are widely achievable

in passive optical nanodevices. Indeed, this proposes a new approach for ultrathin optical isolation of signal.

2. Eigenmodes, Interference, and Fano Resonances

It was recently demonstrated that Fano resonances can lead to circular dichroism in the absorption cross-section of planar chiral nanostructures [11]. The existence of such circular dichroism means that the absorption in the nanostructure was not constrained by reciprocity. In this article, we investigate further Fano resonances and their role in producing nonreciprocal absorption and scattering cross-sections of finite nanostructures. Below, we outline our approach and establish why Fano resonances can be associated with nonorthogonal eigenmodes. The existence of such nonorthogonal eigenmodes is then used to predict and demonstrate propagation-dependent absorption and scattering cross-sections.

The fields inside nanostructures can be associated with the induced currents and polarizations, which determine the complete near- and far-fields produced by the given configuration. In this approach all eigenmodes are defined within finite volumes. However, importantly, there is also a one-to-one correspondence between such eigenmodes and resonances [12], which provides an intuitive basis to capture the optical features of resonant nanostructures. The relationship between induced current, \mathbf{J} , and an arbitrary applied field, \mathbf{E}_0 , is expressible in terms of dyadic Green's functions [13]:

$$-i\omega[\epsilon - \epsilon_0] \mathbf{E}_0(\mathbf{x}) = \mathbf{J}(\mathbf{x}) - k^2[\epsilon(\mathbf{x}) - \epsilon_0] \int_V \hat{\mathbf{G}}_0(\mathbf{x}, \mathbf{x}') \mathbf{J}(\mathbf{x}') d^3x' \tag{1}$$

where k is the wavenumber, ω is the angular frequency, V is the volume of the scatterer (assumed finite), and $\hat{\mathbf{G}}_0$ is the free space dyadic Green's function:

$$\hat{\mathbf{G}}_0(\mathbf{x}, \mathbf{x}') = \text{P.V.} \left[\hat{\mathbf{I}} + \frac{1}{k^2} \nabla \nabla \right] \frac{e^{ik|\mathbf{x}-\mathbf{x}'|}}{4\pi\epsilon_0 |\mathbf{x} - \mathbf{x}'|} - \hat{\mathbf{L}} \frac{\delta(\mathbf{x} - \mathbf{x}')}{k^2\epsilon_0} \tag{2}$$

where $\hat{\mathbf{L}}$ is the source dyadic [13] and P.V. implies a principal value exclusion of $\mathbf{x}' = \mathbf{x}$ when performing the integration in Equation (1). We have also defined permittivity (ϵ) in terms of both the conductivity (σ) and the electric susceptibility (χ) to define the current (\mathbf{J}) as the sum of both polarization and conduction current, which is related to the total electric field as:

$$\epsilon \equiv (\chi + 1)\epsilon_0 - \frac{\sigma}{i\omega} \Rightarrow \mathbf{J}(\mathbf{x}) = -i\omega [\epsilon(\mathbf{x}) - \epsilon_0] \mathbf{E}(\mathbf{x}) \tag{3}$$

Equation (1) is therefore a general expression for modeling the complete optical response of an arbitrary scattering geometry. An eigenmode, \mathbf{v}_i , of any given structure can then be defined such that it will satisfy Equation (1) as:

$$-i\omega[\epsilon - \epsilon_0] \lambda_i \mathbf{v}_i(\mathbf{x}) = \mathbf{J}(\mathbf{x}) - k^2[\epsilon - \epsilon_0] \int_V \hat{\mathbf{G}}_0(\mathbf{x}, \mathbf{x}') \mathbf{v}_i(\mathbf{x}') d^3x' \tag{4}$$

where λ_i is the eigenvalue of \mathbf{v}_i . Because the full set of these eigenmodes form a complete basis for the optical response, they allow us to model the entire range of bright and dark resonances in any given system. However, recently, it was demonstrated that such a basis of eigenmodes is not necessarily orthogonal [14]. The origin of such nonorthogonal eigenmodes can be understood as a consequence of the inherent radiation losses, where the Equation (1) corresponds to a non-Hermitian system. To consider the effect of this nonorthogonality, and its relation to the Fano resonances, we can refer to the extinction cross-section, which can be written in terms of the near-field overlap of induced current and incident field [11,15].

$$\sigma_{\text{ext}} = \frac{1}{|\mathbf{E}_0|^2} \sqrt{\frac{\mu_0}{\epsilon_0}} \operatorname{Re} \left[\int_{V_s} \mathbf{E}_0^* \cdot \mathbf{J} \, dV \right] \tag{5}$$

Additionally, an arbitrary applied field and the induced currents can be defined in terms of a linear superposition of the eigenmodes:

$$\mathbf{E}_0 = \sum_i a_i \lambda_i \mathbf{v}_i \quad \Rightarrow \quad \mathbf{J} = \sum_i a_i \mathbf{v}_i \tag{6}$$

Using these expressions, we are able to rewrite the total extinction (Equation 5) in terms of eigenmodes and eigenvalues:

$$\sigma_{\text{ext}} = \frac{1}{|\mathbf{E}_0|^2} \sqrt{\frac{\mu_0}{\epsilon_0}} \sum_i \left(\underbrace{\operatorname{Re}[\lambda_i] \left(\int_{V_s} |a_i|^2 |\mathbf{v}_i|^2 \, dV \right)}_{\text{direct terms}} + \sum_{j \neq i} \underbrace{\operatorname{Re} \left[a_i^* a_j \lambda_i^* \left(\int_{V_s} \mathbf{v}_i^* \cdot \mathbf{v}_j \, dV \right) \right]}_{\text{interference terms}} \right) \tag{7}$$

Notably, we have two sets of terms contributing to extinction: direct terms that provide contributions to extinction from individual eigenmodes, and also interference terms coming from the overlap between different eigenmodes. For orthogonal eigenmodes the interference term vanishes. Moreover, the presence of nonorthogonal eigenmodes leads to existence of the Fano resonances in this model. To demonstrate this, we first rule out any dependency of a given eigenmode’s excitation (*i.e.*, the a_i coefficients of Equation (6)) on the excitations of other eigenmodes. This can be done very directly, because the dyadic Greens function is complex symmetric

$$\hat{\mathbf{G}}_0(\mathbf{x}, \mathbf{x}') = \hat{\mathbf{G}}_0(\mathbf{x}', \mathbf{x}), \quad \hat{\mathbf{G}}_0 = \hat{\mathbf{G}}_0^T \tag{8}$$

Due to this symmetry, it is possible to write the overall operator of the eigenvalue equation (Equation (4)) as a complex symmetric matrix and in the normal form shown by Gantmacher [16]. Thus, such nondegenerate eigenmodes must be orthogonal under unconjugated projections [17].

$$\int_V \mathbf{v}_\alpha \cdot \mathbf{v}_\beta \, dV = 0 \quad \text{when } \lambda_\alpha \neq \lambda_\beta \tag{9}$$

Subsequently, the excitation of any given eigenmode is defined *entirely* by the eigenmode itself and the incident field:

$$\lambda_i a_i = \frac{\int_V \mathbf{v}_i \cdot \mathbf{E}_0 \, dV}{\int_V \mathbf{v}_i \cdot \mathbf{v}_i \, dV} \tag{10}$$

It shows that the excitation of any given eigenmode is independent from the excitations of any other eigenmode. This means that the only way an interaction between two or more eigenmodes affects the extinction is due to nonorthogonality of these eigenmodes resulting in the interference terms seen Equation (5). This is indeed the conclusion of earlier work for the Fano resonances arising in nanoparticle oligomers [14]. In particular, we have established that the excitation of eigenmodes is determined *entirely* from the eigenmode itself and the excitation field. As such, the unambiguous conclusion is that *all* optical Fano resonances can be considered as a consequence of interference between so-called “bright” eigenmodes. This is in good accordance with the bright mode Fano resonances that have been proposed and observed in recent years [14,18–20]. Furthermore, the existence of nonorthogonal eigenmodes allows us to describe nonreciprocal absorption and scattering cross-sections of lossy nanoscale structures.

3. Nonreciprocal Absorption and Scattering

We begin this section by considering three-dimensional geometries that have at least 3-fold discrete rotational symmetry and are excited by plane waves at normal incidence in order to utilize derivations provided in Ref. [11]. However, the use of such symmetry also prevents any circular cross polarization in transmission [21], which is often observed as circular conversion dichroism [22–24], and not of interest here. Using more formal notation, we focus on structures with C_n symmetry for $n \geq 3$. Notably, unlike the case of planar structures considered in Ref. [11], we do not have a plane of reflection symmetry perpendicular to the propagation direction and we, therefore, cannot relate the excitations of plane waves propagating in opposite directions. As such, we are automatically driven to account for the role of propagation direction. So, we begin by defining the current distribution, \mathbf{J} , induced by a plane wave \mathbf{E}_0 , and a current distribution, \mathbf{J}' , induced by the reciprocal plane wave, \mathbf{E}_0^* , where the * indicates a complex conjugate. These are source and response distributions satisfying Equation (1).

However, we can now acknowledge that a normally-incident plane wave can only excite eigenmodes that transform according to the two-dimensional, E irreducible representations of the rotational symmetry point group (e.g., see Table 1). A result from Ref. [11] then follows directly: if we assume the eigenmodes are orthogonal, then the total current intensity is conserved in the structure between reciprocal plane waves.

$$\int_V \mathbf{J}^* \cdot \mathbf{J} \, dV = \int_V \mathbf{J}'^* \cdot \mathbf{J}' \, dV \tag{11}$$

Table 1. Character table for the 4-fold rotational symmetry group (C_4). Rows are irreducible representations, columns are symmetry operations, and each element denotes the trace of the associated symmetry operation’s matrix representation in the given irreducible representation.

C_4	E	C_4	C_2	C_4^3
A	1	1	1	1
B	1	−1	1	−1
E	$\left\{ \begin{array}{l} 1 \\ 1 \end{array} \right.$	$\left\{ \begin{array}{l} i \\ -i \end{array} \right.$	−1	−1
			−1	i

If we have a uniform material loss throughout our geometry, this result means that the absorption cross-section is conserved for reciprocal planewaves. Thus, due to the fact that the extinction is already conserved by reciprocity, the scattering cross-section must too be conserved, as it is simply the difference between extinction and absorption. In other words, this result shows that nonorthogonal eigenmodes are necessary to permit nonreciprocal behavior in the absorption and scattering cross-sections. In practical terms, we need a structure that can exhibit a Fano resonance under plane wave excitation. Now, if we are considering a single, isotropic and homogeneous material, the eigenmodes of the Green’s function operator (depicted in Equation (1)) are the eigenmodes of the total system. The eigenmodes are therefore independent of material properties, which instead affect only the eigenvalues. Notably, \hat{G}_0 is a complex symmetric operator, which means that, when \hat{G}_0 is real, the whole operator is actually real symmetric and therefore *Hermitian*; making all its eigenmodes orthogonal. As the source dyadic (\hat{L}) is real, this means that retardation of coupling within the structure has to be nontrivial ($e^{ik|x-x'|} \not\rightarrow 1$) in order to have nonorthogonal eigenmodes. This retardation condition provides a design guideline for generation of the Fano resonances. Nanoparticle oligomers were used as planar chiral geometries to satisfy this retardation condition in Ref. [11], but for nonplanar geometries we can instead look to the work done in the area of stereometamaterials [25]; three-dimensional structures commonly, albeit not always [26], constructed from stacked elements [27–29]. Here, the distance between stacked elements is able to guarantee nontrivial retardation in coupling.

To demonstrate that this indeed provides nonorthogonal eigenmodes, we consider a simple dimer model of two electric dipoles, \mathbf{p}_1 and \mathbf{p}_2 , with isotropic polarizabilities, α_1 and α_2 , at locations, \mathbf{r}_1 and \mathbf{r}_2 , along a principal axis, separated by a distance, $|\mathbf{r}_1 - \mathbf{r}_2| = d$. For such a system, we can use the relation between current and polarization in Equation (3), to simplify Equation (1) down to the known dipole model.

$$\alpha_1 \epsilon_0 \mathbf{E}_0(\mathbf{r}_1) = \mathbf{p}_1 - \alpha_1 k^2 \hat{G}_0(\mathbf{r}_1, \mathbf{r}_2) \mathbf{p}_2 \tag{12}$$

$$\alpha_2 \epsilon_0 \mathbf{E}_0(\mathbf{r}_2) = \mathbf{p}_2 - \alpha_2 k^2 \hat{G}_0(\mathbf{r}_2, \mathbf{r}_1) \mathbf{p}_1 \tag{13}$$

Given the reflection symmetry of the structure about the principal axis, there will be one set of eigenmodes with dipole moments polarized parallel to the principal axis and a separate (orthogonal) set

of eigenmodes that have dipole moments polarized perpendicular to the principal axis. This orthogonal separation is a result of the eigenmodes that are affected by such symmetric reflection operations being orthogonal to those that are not affected. More formally, it is a consequence of the eigenmodes being associated with different irreducible representations of the $C_{\infty v}$ point group. In any case, we are able to consider exclusively the dipole moments that are perpendicular to the principal axis, because they correspond to those that can be excited by a plane wave propagating along the principal axis. Moreover, the relationship between these dipole moments and the applied field can be written in a simplified form:

$$\mathbf{E}_0(\mathbf{r}_1) = (\alpha_1\epsilon_0)^{-1}\mathbf{p}_1 - G_d\mathbf{p}_2 \tag{14}$$

$$\mathbf{E}_0(\mathbf{r}_2) = (\alpha_2\epsilon_0)^{-1}\mathbf{p}_2 - G_d\mathbf{p}_1 \tag{15}$$

$$\text{where } G_d \equiv \frac{e^{ikd}}{4\pi\epsilon_0 d} \left(k^2 + \frac{ik}{d} - \frac{1}{d^2} \right)$$

From this, we can deduce analytical expressions for the two nondegenerate eigenmodes that are excitable by a planewave in this system:

$$|\mathbf{v}_{1,2}\rangle \equiv \begin{bmatrix} \mathbf{p}_1 \\ \mathbf{p}_2 \end{bmatrix} = \begin{bmatrix} \alpha_2 - \alpha_1 \pm \delta \\ 2\alpha_1\alpha_2\epsilon_0 G_d \end{bmatrix} \tag{16}$$

$$\text{where } \delta \equiv \sqrt{(\alpha_2 - \alpha_1)^2 + (2\alpha_1\alpha_2\epsilon_0 G_d)^2}$$

Importantly, these two eigenmodes are not necessarily orthogonal provided that $\alpha_1 \neq \alpha_2$ and $G_d \neq 0$,

$$\langle \mathbf{v}_1 | \mathbf{v}_2 \rangle = |2\alpha_1\alpha_2\epsilon_0 G_d|^2 + (\alpha_2 - \alpha_1 + \delta)^* \cdot (\alpha_2 - \alpha_1 - \delta) \tag{17}$$

Therefore, these results demonstrate that nonorthogonal eigenmodes exist even in the dimer model, but only if there is coupling between the dipoles and the dipole polarizabilities are different. In other words, Equation (17) suggests that even an asymmetric dimer should be able to realize nonorthogonal eigenmodes and, therefore, nonreciprocal absorption and scattering. To demonstrate this, we consider an idealized dimer made from two nanoparticles of 200 nm diameter. We also assume that the material properties of nanoparticles are described by Drude model with a plasma frequency of 2.07 PHz. The particles are separated by a gap of 200 nm and excited with a plane wave along the dimer’s principal axis. This structure is illustrated in Figure 2a. The nonreciprocal absorption can be obtained by making one particle lossless and the other particle lossy with a damping factor of 600 THz (a very large damping). Importantly, because we define one nanosphere to be lossless, the absorption cross-section will only be related to the dipole moment intensity in the lossy particle, and not the integral over the complete geometry that we originally considered for continuous systems made from a single material, such as in Equation (11).

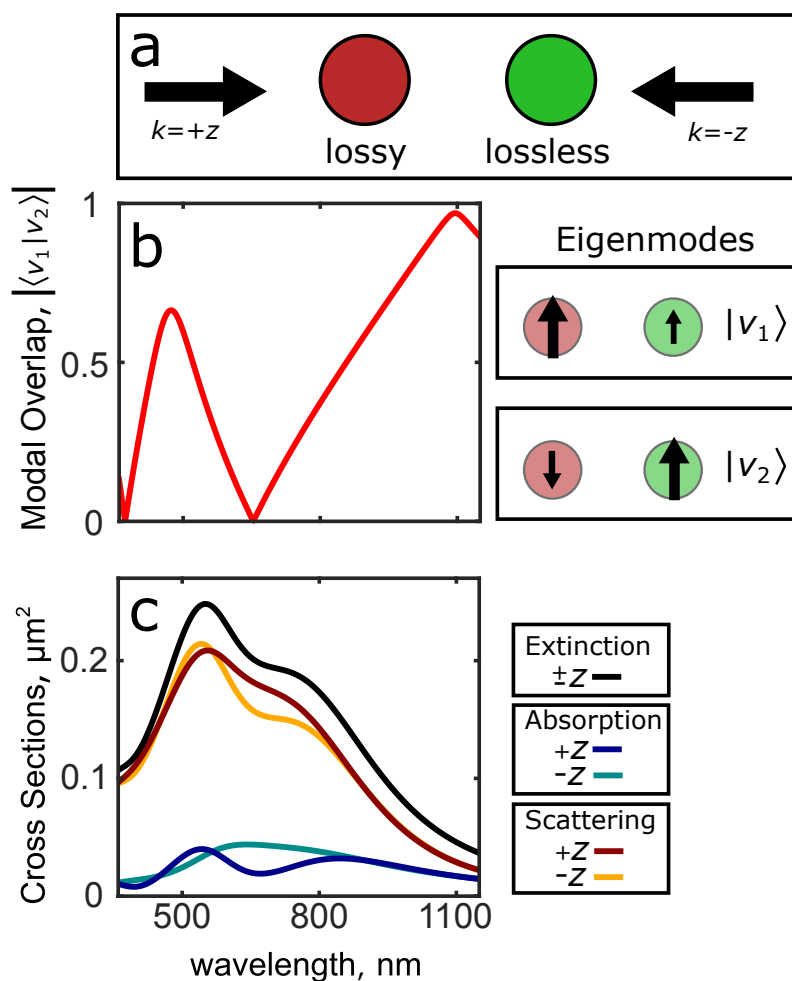


Figure 2. (a) Schematic of the system under consideration: a dimer consisting of lossy and lossless nanoparticles excited by plane waves propagating in opposite directions along the dimer’s principal axis. The parameters are in the text. We plot (b) the absolute value of the projection (Equation (17)) between the two normalized eigenmodes (Equation (16)) of this geometry. The simulated extinction, absorption and scattering cross-sections show the associated difference for oppositely-propagating plane waves.

In Figure 2b, we show that the dipole model eigenmodes of this dimer (Equation (16)) are nonorthogonal across the majority of the visible frequency range. The extinction, absorption and scattering cross-sections of this dimer are then shown in Figure 2c. It demonstrates the difference in the scattering and absorption between oppositely-propagating planewaves at wavelengths where two resonances appear to overlap. Thus, even such a simple dual-layer geometry is able to provide strongly nonorthogonal eigenmodes and the nonreciprocal behavior. Notably, while we utilized different materials to produce nonorthogonal eigenmodes for this dimer, the coupling between dipoles is still a necessity for nonorthogonal eigenmodes (*i.e.*, consider $G_d \rightarrow 0$ in Equation (17)). However, to consider a realistic dimer nanostructure, we have to acknowledge that material properties are largely fixed by fabrication and that we must instead consider geometry. On the simplest level, different sizes and shapes of nanoparticles will be associated with different dipole polarizabilities and thereby produce the same effect as material change did in Figure 2. Ultimately, the dipole responses in a nanoparticle

dimer do not provide sufficient freedom to induce significant modal interference with realistic material parameters. We can optimize the response by considering pairs of stacked, symmetric nanocrosses as seen in Figure 3 (similar in concept to the stereometamaterial in Ref. [27]). Arrays of such stacked nanocross geometries have previously exhibited a difference in effective impedance and hence reflection for opposite propagation directions [30]. For our analysis, a relative twist in the orientations of the nanocrosses also provides chirality and allows us to consider the lowest symmetry conditions that our earlier theoretical arguments applied to (*i.e.* the C_n point groups).

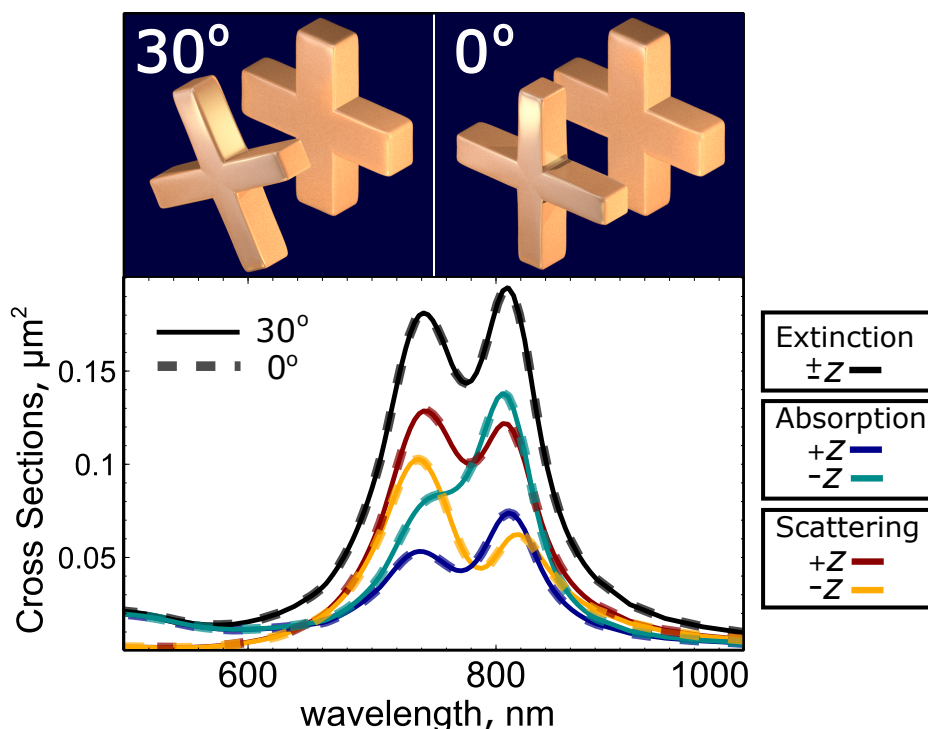


Figure 3. Simulated nonreciprocal scattering and absorption cross-sections in stacked gold nanocrosses from linearly-polarized plane waves propagating in opposite directions ($\pm z$) along the rotational symmetry axis. Simulation results are shown to be the same for both chiral (C_4) and achiral (C_{4v}) structures, and both are independent of polarization. The calculation parameters are given in the text.

The dimensions of the stacked nanocrosses were chosen as to produce nonorthogonal eigenmodes and a Fano resonance by pushing the independent resonances of each nanocross together. This is done in Figure 3 using a pair of gold crosses separated by a 120 nm gap, and with dimensions: total length equal to 150 nm, arm width equal to 40 nm and thickness equal to 30 nm. We then reduced the arm width, w , of one cross to 25 nm in order to provide the necessary asymmetry. In Figure 3, we can clearly see that the absorption and scattering cross-sections differ dramatically between reciprocal plane waves, and independently of whether the structure is chiral or not. Interestingly, the lack of chirality tells us that the difference in scattering and absorption cannot be attributed to bianisotropic coupling, which was the mechanism for the impedance difference in Ref. [30]. In this regard, the symmetry of the individual crosses ensures that, in isolation, their optical responses are isotropic, yet notably: the optical response of the stacked crosses remains independent to the relative twist, which suggests that there is isotropic coupling between the two crosses. Such isotropic coupling would exist if the dominant

interaction between crosses was dipolar, as it would make the situation analogous to the coupled isotropic dipoles considered for Figure 2. Dipolar coupling would be expected to dominate with increasing separation between crosses, and, therefore, the twist-independent optical response we observe will be a consequence of the larger distance between the two crosses. Additionally, as is also suggested by the negligible effect of chirality, the choice of linear or circular polarization of the incident plane wave has no effect on any of the cross-sections. Indeed, in the chiral geometry, there appears to be negligible circular dichroism between oppositely-handed plane waves that propagate in the same direction for any of the cross-sections, simply because the associated curves are separated by less than $0.001 \mu\text{m}^2$. Similarly, in regard to linear polarizations, the angle of linear polarization is of no significance because the discrete rotational symmetry is separately known to prevent any such angular dependence in *all* of the cross-sections [31]. Figure 3 therefore demonstrates that Fano resonances and modal interference in stacked nanocross geometries allow for significant variation in optical response depending on the propagation direction and irrespective of *any* polarization. All simulations were performed using CST Microwave Studio and gold data was taken from Johnson and Christy [32].

To finally provide an investigation into the role of the asymmetry about the z -axis for these stacked nanocrosses, we can consider varying the arm width, w , of one nanocross while holding the other constant. The absorption, scattering and extinction cross-sections of the stacked nanocrosses through this parameter sweep are shown in Figure 4. Notably, when the two nanocrosses are identical ($w = 40 \text{ nm}$), the geometry has D_4 symmetry and is, thereby, invariant under a π -rotation perpendicular to the principal rotation axis, which makes reciprocal planewaves equivalent under geometric symmetry operations. In other words, we cannot have D_n symmetry if we want to produce nonreciprocal absorption and scattering. However, we can see that this invariance is related to direction of scattering and absorption splitting interchanging either side of D_n symmetry. Therefore, Figure 4 ultimately shows us that the difference in scattering and absorption is widely achievable in systems such as stacked nanocrosses that support closely overlapped and coupled resonances, and therefore modal interference. As such, this demonstrates that significant nonreciprocal measurements can be performed with stereometamaterial geometries.

4. Conclusions

We have shown that the distinct absorption and scattering cross-sections of nonplanar nanostructures can distinguish between reciprocal planewaves, provided the system has nonorthogonal eigenmodes. The relation of this effect to nonorthogonal eigenmodes was derived rigorously, and subsequently we established that the nonreciprocal absorption and scattering could be realized and enhanced through the Fano resonances. We have proposed that two stacked nanocrosses would provide the necessary retarded coupling to produce nonorthogonal eigenmodes and, thus, Fano resonances, while also providing sufficient design freedom for optimization. It was subsequently demonstrated that this geometry produces substantial differences in absorption and scattering cross-sections for plane waves that propagate in opposite directions. It was additionally shown that this difference would be independent of the plane wave's polarization. This work subsequently establishes that modal interference and

Fano resonances enable a passive nanostructure to simultaneously measure and distinguish signal from reciprocal plane waves.

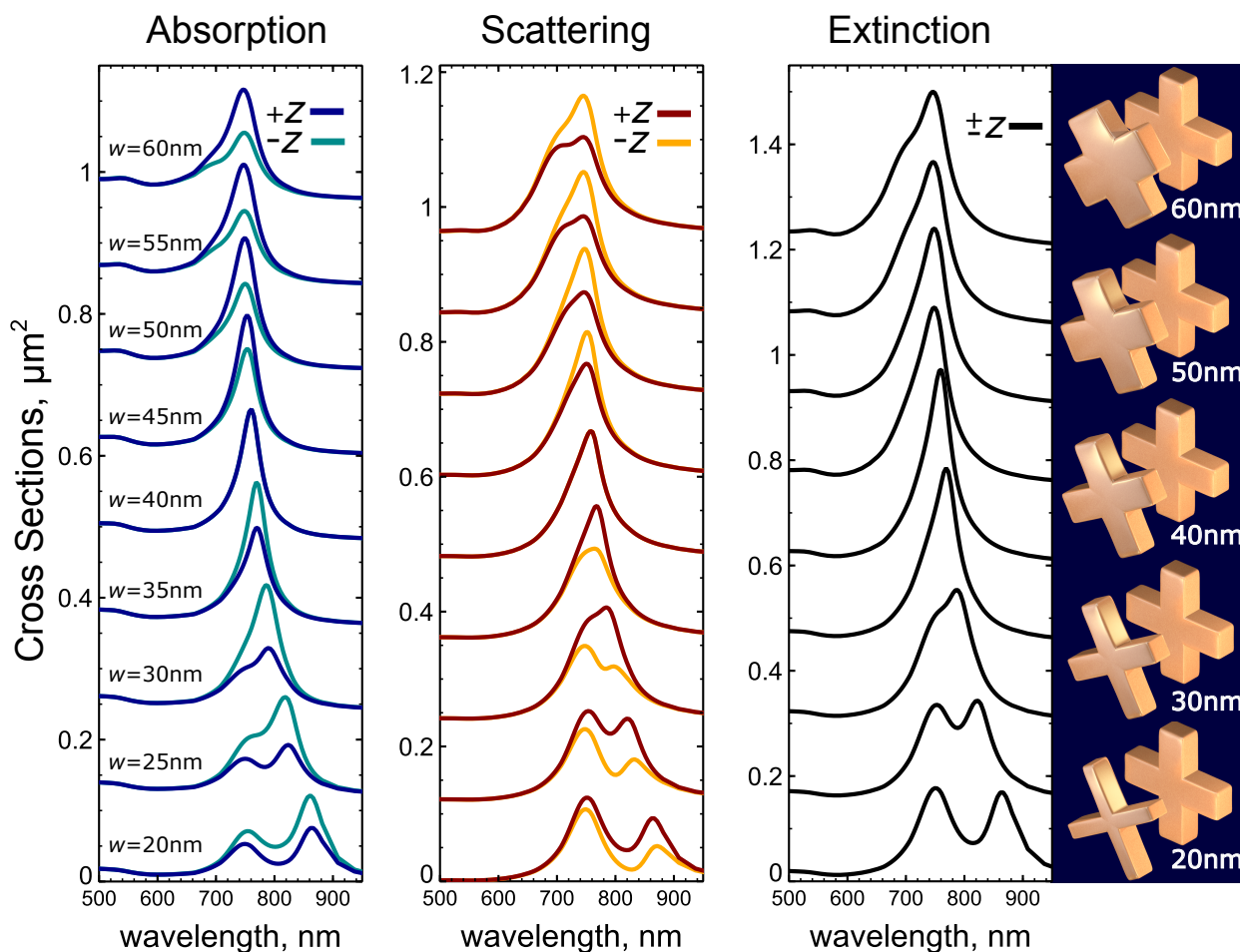


Figure 4. Simulation results for stacked gold nanocrosses, under excitation from circularly polarized plane waves given by propagation in either the +z or -z direction. The variation between right and left circular polarizations in the same propagation direction is negligible ($< 0.001\mu\text{m}^2$) and making the associated curves overlapped here. The arm width, w , of one nanocross arm is varied from 20 to 60 nm, showing a significant difference in the absorption and scattering cross-section of reciprocal planewaves, provided the system does not have D_4 symmetry. The calculation parameters are given in text.

Acknowledgments

This work was supported by the Australian Research Council. ANP acknowledges support of the Russian Foundation for Basic Research and the Deutsche Forschungsgemeinschaft in the frame of International Collaborative Research Center TRR 160. BH would like to acknowledge the productive discussions with David A. Powell on eigenmodes, complex symmetric operators and bianisotropy in twisted crosses.

Author Contributions

BH, AEM and ANP developed the theory. AEM and YSK supervised the research. BH, AEM and YSK wrote the manuscript.

Conflicts of Interest

The authors declare no conflict of interest.

References

1. Saxon, D.S. Tensor Scattering Matrix for the Electromagnetic Field. *Phys. Rev.* **1955**, *100*, 1771–1775.
2. Mishchenko, M.I.; Travis, L.D.; Lacis, A.A. *Scattering, Absorption, and Emission of Light by Small Particles*; Cambridge University Press: Cambridge, UK, 2002.
3. Raab, R.E.; de Lange, O.L. *Multipole Theory in Electromagnetism*; Oxford University Press: Oxford, UK, 2005.
4. Zhao, R.; Koschny, T.; Soukoulis, C.M. Chiral metamaterials: Retrieval of the effective parameters with and without substrate. *Opt. Express* **2010**, *18*, 14553–14567.
5. Wen, C.P. Coplanar Waveguide: A Surface Strip Transmission Line Suitable for Nonreciprocal Gyromagnetic Device Applications. *IEEE Trans. Microw. Theory Techn.* **1969**, *17*, 1087–1090.
6. Figotin, A.; Vitebsky, I. Nonreciprocal magnetic photonic crystals. *Phys. Rev. E* **2001**, *63*, 066609.
7. Potton, R.J. Reciprocity in optics. *Rep. Prog. Phys.* **2004**, *67*, 717–754.
8. Bi, L.; Hu, J.; Jiang, P.; Kim, D.H.; Dionne, G.F.; Kimerling, L.C.; Ross, C.A. On-chip optical isolation in monolithically integrated non-reciprocal optical resonators. *Nat. Photon.* **2011**, *5*, 758–762.
9. Mousavi, S.H.; Khanikaev, A.B.; Allen, J.; Allen, M.; Shvets, G. Gyromagnetically Induced Transparency of Metasurfaces. *Phys. Rev. Lett.* **2014**, *112*, 117402.
10. Kim, J.; Kuzyk, M.C.; Han, K.; Wang, H.; Bahl, G. Non-reciprocal Brillouin scattering induced transparency. *Nat. Phys.* **2015**, *11*, 275–280.
11. Hopkins, B.; Hwang, Y.; Poddubny, A.N.; Miroshnichenko, A.E.; Davis, T.J.; Kivshar, Y.S. Circular dichroism induced by Fano resonances in planar chiral oligomers. *arXiv* **2014**.
12. Powell, D.A. Resonant dynamics of arbitrarily shaped meta-atoms. *Phys. Rev. B* **2014**, *90*, 075108.
13. Yaghjian, A.D. Electric Dyadic Green's Functions in the Source Region. *Proc. IEEE* **1980**, *68*, 248–263.
14. Hopkins, B.; Poddubny, A.N.; Miroshnichenko, A.E.; Kivshar, Y.S. Revisiting the physics of Fano resonances for nanoparticle oligomers. *Phys. Rev. A* **2013**, *88*, 053819.
15. Merchiers, O.; Moreno, F.; Gonzalez, F.; Saiz, J.M. Light scattering by an ensemble of interacting dipolar particles with both electric and magnetic polarizabilities. *Phys. Rev. A* **2007**, *76*, 043834.
16. Gantmacher, F. *The Theory of Matrices*; Chelsea Publishing Company: New York, NY, USA, 1959.

17. Craven, B. Complex Symmetric Matrices. *J. Austral. Math. Soc.* **1969**, *10*, 341–354.
18. Frimmer, M.; Coenen, T.; Koenderink, A.F. Signature of a Fano Resonance in a Plasmonic Metamolecule's Local Density of Optical States. *Phys. Rev. Lett.* **2012**, *108*, 077404.
19. Lovera, A.; Gallinet, B.; Nordlander, P.; Martin, O.J. Mechanisms of Fano Resonances in Coupled Plasmonic Systems. *ACS Nano* **2013**, *7*, 4527–4536.
20. Forestiere, C.; Negro, L.D.; Miano, G. Theory of coupled plasmon modes and Fano-like resonances in subwavelength metal structures. *Phys. Rev. B* **2013**, *88*, 155411.
21. Fernandez-Corbaton, I. Forward and backward helicity scattering coefficients for systems with discrete rotational symmetry. *Opt. Express* **2013**, *21*, 29885.
22. Schwanecke, A.S.; Fedotov, V.A.; Khardikov, V.V.; Prosvirnin, S.L.; Chen, Y.; Zheludev, N.I. Nanostructured metal film with asymmetric optical transmission. *Nano Lett.* **2008**, *8*, 2940–2943.
23. Plum, E.; Zheludev, N.I. Chirality and anisotropy of planar metamaterials. In *Structured Surfaces as Optical Metamaterials*; Cambridge University Press: Cambridge, UK, 2011; pp. 94–157.
24. Plum, E.; Fedotov, V.A.; Zheludev, N.I. Asymmetric transmission: A generic property of two-dimensional periodic patterns. *J. Opt.* **2011**, *13*, 024006.
25. Liu, N.; Liu, H.; Zhu, S.; Giessen, H. Stereometamaterials. *Nat. Phot.* **2009**, *3*, 157–162.
26. Frank, B.; Yin, X.; Schäferling, M.; Zhao, J.; Hein, S.M.; Braun, P.V.; Giessen, H. Large-Area 3D Chiral Plasmonic Structures. *ACS Nano* **2013**, *7*, 6321–6329.
27. Decker, M.; Ruther, M.; Krieglner, C.E.; Zhou, J.; Soukoulis, C.M.; Linden, S.; Wegener, M. Strong optical activity from twisted-cross photonic metamaterials. *Opt. Lett.* **2009**, *34*, 2501–2503.
28. Decker, M.; Zhao, R.; Soukoulis, C.M.; Linden, S.; Wegener, M. Twisted split-ring-resonator photonic metamaterial with huge optical activity. *Opt. Lett.* **2010**, *35*, 1593–1595.
29. Hentschel, M.; Schaeferling, M.; Metzger, B.; Giessen, H. Plasmonic Diastereomers: Adding up Chiral Centers. *Nano Lett.* **2012**, *13*, 600–606.
30. Hannam, K.; Powell, D.A.; Shadrivov, I.V.; Kivshar, Y.S. Broadband chiral metamaterials with large optical activity. *Phys. Rev. B* **2014**, *89*, 125105.
31. Hopkins, B.; Liu, W.; Miroshnichenko, A.E.; Kivshar, Y.S. Optically isotropic responses induced by discrete rotational symmetry of nanoparticle clusters. *Nanoscale* **2013**, *5*, 6395–6403.
32. Johnson, P.B.; Christy, R.W. Optical Constants of the Noble Metals. *Phys. Rev. B* **1972**, *6*, 4370–4379.